Magnetic field tuning of parallel spin stripe order and fluctuations near the pseudogap quantum critical point in $La_{1.36}Nd_{0.4}Sr_{0.24}CuO_4$

Qianli Ma ◉,[1] Evan M. Smith ◉,[1] Zachary W. Cronkwright ◉,[1] Mirela Dragomir ◉,[2,3] Gabrielle Mitchell,[1] Barry W. Winn ◉,[4] Travis J. Williams,[4] and Bruce D. Gaulin[1,2,5]

[1]*Department of Physics and Astronomy, McMaster University, Hamilton, Ontario, Canada L8S 4M1*
[2]*Brockhouse Institute for Materials Research, Hamilton, Ontario, Canada L8S 4M1*
[3]*Electronic Ceramics Department, Jožef Stefan Institute, 1000 Ljubljana, Slovenia*
[4]*Neutron Scattering Division, Oak Ridge National Laboratory, Oak Ridge, Tennessee 37830, USA*
[5]*Canadian Institute for Advanced Research, MaRS Centre, West Tower 661 University Ave., Suite 505, Toronto, Ontario, Canada M5G 1M1*

A quantum critical point in the single-layer, hole-doped cuprate system $La_{1.6-x}Nd_{0.4}Sr_xCuO_4$ (Nd-LSCO) near $x = 0.23$ has been proposed as an organizing principle for understanding high-temperature superconductivity. Our earlier neutron diffraction work on Nd-LSCO at optimal and high doping revealed static parallel spin stripes to exist out to the quantum critical point and slightly beyond, at $x = 0.24$ and 0.26. We examine more closely the parallel spin stripe order parameter in Nd-LSCO in both zero magnetic field and fields up to 8 T for $H \parallel c$ in these single crystals. In contrast to earlier studies at lower doping, we observe that $H \parallel c$ in excess of ~2.5 T eliminates the incommensurate quasi-Bragg peaks associated with parallel spin stripes. But this elastic scattering is not destroyed by the field; rather it is transferred to commensurate $\mathbf{Q} = \mathbf{0}$ Bragg positions, implying that the spins participating in the spin stripes have been polarized. Inelastic neutron scattering measurements at high fields show an increase in the low-energy, parallel spin stripe fluctuations and evidence for a spin gap $\Delta_{\text{spin}} = 3 \pm 0.5$ meV for Nd-LSCO with $x = 0.24$. This is shown to be consistent with spin-gap measurements as a function of superconducting T_C over five different families of cuprate superconductors, which follow the approximate linear relation $\Delta_{\text{spin}} = 3.5 k_B T_C$.

I. INTRODUCTION

Quasi-two-dimensional (2D) high-temperature superconducting cuprates have been of intense interest since their discovery some 35 years ago [1–16]. A central dimension to their behavior has been the relationship between antiferromagnetism and superconductivity and how this evolves with hole doping, as occurs when Sr^{2+} is substituted for La^{3+} in either $La_{2-x}Sr_xCuO_4$ (LSCO) or $La_{1.6-x}Nd_{0.4}Sr_xCuO_4$ (Nd-LSCO), or when with Ba^{2+} is substituted for La^{3+} in $La_{2-x}Ba_xCuO_4$ (LBCO) [17,18]. The undoped parent compound of this single-layer, 214 family of cuprate superconductors is La_2CuO_4, a Mott insulator which displays commensurate, three-dimensional (3D) antiferromagnetic (AF) order at ~300 K [19,20]. Doping with mobile holes quickly destroys the 3D AF order, at $x \sim 0.2$, replacing it with quasi-2D incommensurate order, that can be described within the stripe model [18,21]. Superconductivity first appears at $x = 0.05$, but the superconducting phase diagram is structured as a function of hole doping x, with a depression in T_C at the "$\frac{1}{8}$ anomaly," $x = 0.125$, and superconducting ground states extend out to at least $x \sim 0.27$ [22,23].

Describing the 2D CuO_2 layers as edge-sharing squares for which the tetragonal $a = b = 3.88$ Å lattice constants are Cu-Cu near-neighbor distances, the AF structure in the absence of holes is a "π, π" Neel state with commensurate magnetic Bragg peaks at the $(\frac{1}{2}, \frac{1}{2}, 0)$ positions in reciprocal space. Within the stripe model, mobile holes are accommodated inhomogeneously, with the holes being organized into quasi-1D charge stripes, separating regions that locally resemble the "π, π" Neel state. However, the charge stripes introduce a π phase shift between local Neel states on either side of them, resulting in a 2D incommensurate magnetic structure. As such, the stripe model interleaves incommensurate charge order with incommensurate spin order, and the π phase shift between local "π, π" Neel states across the charge stripes implies that the incommensuration of the charge stripes is double that of the spin stripes [18,21,24–28].

A theory framework for understanding the commensurability between spin and charge stripes was introduced some time ago [26]. It is worth noting, however, that this is only observed at low temperatures and in the 214 single-layer family of cuprate superconductors. In other families of high-T_C cuprates, such stripe ordered states are not commensurate with each other and even appear to inhabit different doping regimes, suggesting competition. A theoretical discussion of this phenomenology has also been presented [27].

Static spin stripe order was first observed by neutron scattering techniques in the Nd-LSCO system at the "$\frac{1}{8}$ anomaly" $x = 0.125$ [21]. The quasi-Bragg peaks so observed were not resolution limited, but displayed four incommensurate magnetic peaks split off from the $(\frac{1}{2}, \frac{1}{2}, 0)$, or $(\pi, \pi, 0)$,
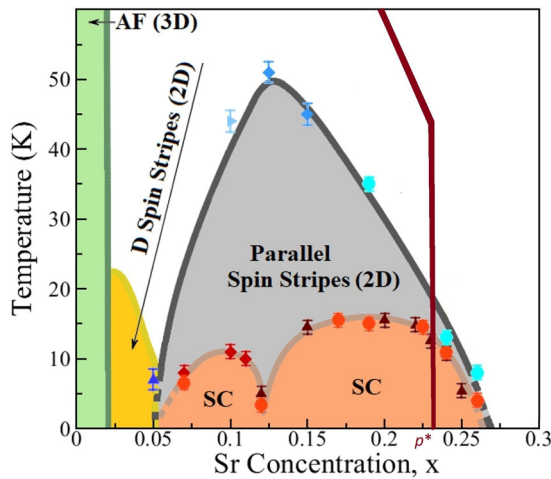
FIG. 1. The magnetic and superconducting phase diagram for Nd-LSCO is shown, along with the line of T^* vs x for the pseudogap phase, which terminates at a quantum critical point, identified in [22] as $x^* = 0.23$. The sample under study in this paper, $x = 0.24$, is immediately to the overdoped side of x^*. This plot is modified from Ref. [32], where the references for the magnetic and superconducting transition temperatures are given.

position in reciprocal space [21]. Two spin stripe structures are observed as a function of hole doping. At low hole doping, $0.02 \leqslant x \leqslant 0.05$, "diagonal spin stripes" are observed and are characterized by quasi-1D charge stripes running along (1,1,0) directions in tetragonal reciprocal space, or next-near-neighbor Cu-Cu directions within the basal plane in real space [29]. A 45° rotation of the spin stripe structure was observed at $x \sim 0.05$, to a "parallel spin stripe" structure, remarkably co-incident with the transition to superconducting ground states [29]. This was first observed in the LSCO family, and was later observed in both LBCO and Nd-LSCO [29–32]. The parallel spin stripe structure displays four quasi-Bragg peaks split off from the $(\pi, \pi, 0)$ position in reciprocal space, at wave vectors $(\frac{1}{2}, \frac{1}{2} \pm \delta, 0)$ and $(\frac{1}{2} \pm \delta, \frac{1}{2}, 0)$. The incommensuration δ obeys the so-called Yamada law at low doping, with $\delta \sim x$, before leveling off beyond the $\frac{1}{8}$ anomaly $x \sim 0.125$ [33].

The Nd-LSCO family has gained much recent attention, primarily because its phase diagram displays the full complexity of cuprate high-temperature superconductivity, while also displaying relatively low superconducting T_C's (maximum $T_C \sim 15$ K), compared to the LSCO and LBCO families (maximum T_C's ~40 and 35 K, respectively) [22,34–36]. Thus, experimentally practical magnetic fields can suppress superconductivity completely in the Nd-LSCO family, and its normal-state properties at optimal and high doping levels can be experimentally explored.

This has proved very useful for exploring the so-called pseudogap phase of Nd-LSCO. Transport and thermodynamic measurements in high magnetic fields have mapped out the boundary of the pseudogap phase in Nd-LSCO [22]. This boundary terminates at p* and is superposed in red on Nd-LSCO's magnetic and superconducting phase diagram in Fig. 1. In particular, strong thermodynamic evidence for a pseudogap quantum critical point (QCP) has been reported in Nd-LSCO near $x \sim 0.23$ [22,35]. This concentration is also

coincident with the closing of an observed antinodal gap in ARPES measurements on Nd-LSCO at $x \sim 0.24$ [37,38]. Furthermore, measurements of the Hall number n_H at low temperatures show a transition from $n_H \sim x$ to $n_H \sim 1 + x$ at $x \sim 0.23$. While there is a compelling case for the existence of a pseudogap QCP in Nd-LSCO near $x \sim 0.23$, the question remains as to whether or not the pseudogap QCP is a key organizing principle in understanding cuprate superconductivity.

Neutron scattering from hole-doped single-layer cuprates in general, and Nd-LSCO in particular, have been limited at optimal and high doping, due to difficulties in growing sufficiently large single crystals to allow such studies. Hence, information on stripe correlations near and through the pseudogap QCP have themselves been limited. However, recent progress has allowed a set of single crystals appropriate for neutron scattering to be grown [23]. Combined with advances in neutron scattering instrumentation, this has allowed the recent study of both the static (on the timescale of the neutron) and dynamic parallel spin stripes in Nd-LSCO at $x = 0.19$, 0.24, and 0.26, which spans doping levels from optimal doping, to the pseudogap QCP, to the approximate end of superconductivity [32,39]. Elastic neutron scattering reports static parallel spin stripes at low temperatures at all three concentrations, but with quasi-Bragg peaks characterized by decreasing in-plane correlation lengths and rapidly decreasing intensities, as a function of x [32]. The temperature dependence of the static parallel spin stripe order, or the order parameters, allow good estimates for 2D $T_N(x)$ and these are plotted in Fig. 1. Inelastic neutron scattering below $\hbar\omega = 35$ meV on the same three single-crystal samples, as well as an additional one at $x = 0.125$, show little change in the dynamic spectral weight of parallel spin stripe fluctuations from $x = 0.125$ to 0.24, followed by an $\sim \frac{1}{3}$ reduction in spectral weight at $x = 0.26$ [39]. There is, therefore, no striking correlation observed between either the static or dynamic parallel spin stripe magnetism and the pseudogap QCP in Nd-LSCO. In LSCO, the dynamic spin fluctuations have also been studied throughout the phase diagram at different energy transfer ranges. Wakimoto *et al.* observed diminished intensities of the parallel spin fluctuations up to 100 meV and $0.25 < x < 0.30$ [40,41]. Recently, Tranquada *et al.* observed a peak in the normal-state spin-fluctuation weight at ~20 meV in both $x = 0.21$ and 0.17 bracketing the QCP in LSCO at $x = 0.19$. This behavior is also inconsistent with quantum critical behavior similar to that in Nd-LSCO [39].

It is therefore important to examine the parallel spin stripe magnetism in Nd-LSCO near the pseudogap QCP in greater detail, and especially how it responds to an applied magnetic field. With that in mind, we have revisited the parallel spin stripe order parameter in our $x = 0.24$ single-crystal sample in zero magnetic field [32], and performed new in-field order parameter measurements in $H \parallel c$ up to 8 T. In this paper we combine these with low-energy, inelastic neutron scattering measurements in $H \parallel c$ capable of examining the spin gap in the $x = 0.24$ sample with $T_C = 11 \pm 1$ K.

The magnetic field dependence of spin and charge stripe order in the 214 family of cuprates has an extensive history, and has been of great topical interest in the past. Lake *et al.* [42] first reported a strong increase in the strength of magnetic quasi-Bragg peaks due to parallel stripe order in the presence

of an applied magnetic field in underdoped LSCO, specifically $x = 0.10$. These well-known results were discussed in the context of the SO(5) theory of superconductivity, where superconducting and magnetic order parameters could be rotated into each other [43]. Later in-field measurements on LSCO with $x = 0.105, 0.12$, and 0.145 largely confirmed this result [44], while measurements on Nd-LSCO for $x = 0.12$ to $H \parallel c = 10$ T [44] and LBCO for $x = 0.125$ to $H \parallel c = 7$ T [45] showed either no field dependence or a slight increase in the parallel spin stripe order parameter on application of the field, respectively.

Neutron diffraction measurements looking at the field dependence of spin and charge stripes were carried out on Nd-LSCO approaching optimal hole doping $x = 0.15$ [46]. In zero magnetic field, the parallel spin stripe order parameter shows an abrupt rise at temperatures below ~ 5 K, due to the onset of Nd^{3+} moments ordering and taking part in the spin stripe order. Measurements in an $H \parallel c = 7$ T field suppress this low-temperature component of the order parameter, and also result in an $\sim 20\%$ reduction in the order parameter at higher temperatures before going to zero at ~ 40 K. A magnetic field scan of the order parameter at very low temperatures, ~ 0.1 K, shows the Nd^{3+}-induced enhancement of the order parameter to be largely eliminated by application of a $H \parallel c \sim 0.7$ T magnetic field. Complementary neutron diffraction measurements of the parallel *charge* stripe order in Nd-LSCO with $x = 0.15$ show no magnetic field dependence up to $H \parallel c = 4$ T [46].

II. EXPERIMENTAL METHODS AND MATERIALS

High-quality single crystals of Nd-LSCO with $x = 0.24$ were grown using the traveling solvent floating zone technique at McMaster University and the resulting single crystals weighed around 4 g. The single crystals were produced using a four-mirror Crystal Systems, Inc., halogen lamp image furnace at approximate growth speeds of 0.68 mm/hr, and growths lasted for approximately 1 week. The Sr concentration of this single crystal was determined by careful correlation of the structural phase transition temperatures with preexisting phase diagrams, as described in [23]. Further details regarding the materials preparation and single-crystal growth of these samples, as well as determination of their stoichiometry, is reported in [23]. The single-crystal sample used in this study displayed a mosaic spread of less than $0.5°$, attesting to their high-quality, single-crystalline nature. This is the same $x = 0.24$ single crystal as was studied earlier in zero field in [32,39]. As reported in Michon *et al.* [22], heat-capacity measurements in a magnetic field $\parallel c$ at low temperatures, $T = 2$ K, show saturation above 8 T in Eu-LSCO $x = 0.24$ and above 9 T in Nd-LSCO $x = 0.23$. Hence, the bulk critical magnetic field $\parallel c$ for Nd-LSCO with $x = 0.24$ at $T = 2$ K is close to 8 T.

Triple-axis neutron scattering measurements were conducted on the HB3 triple-axis spectrometer (TAS) at the High Flux Isotope Reactor of Oak Ridge National Laboratory (ORNL) on the same sample $x = 0.24$ single crystal. The sample was mounted in a pumped ^{4}He refrigerator with a vertical magnetic magnetic field capable of achieving a maximum applied field of 8 T. The single-crystal sample

was aligned with its $HK0$ scattering plane coincident with the horizontal plane, hence the applied magnetic field was applied $\parallel c$. The TAS employed PG002 single crystals as both monochromator and analyzer with collimation of $48'$-$40'$-$40'$-120. The scattered neutron energy was fixed at 14.7 meV, allowing the use of pyrolytic graphite filter in the scattered beam, and the energy resolution [full width at half-maximum (FWHM)] of the TAS measurements performed was 1.1 meV.

Complementary time-of-flight (TOF) neutron spectroscopic measurements were carried out on the $x = 0.24$ single crystal using the direct-geometry, time-of-flight hybrid spectrometer HYSPEC [47], at the Spallation Neutron Source of ORNL. All measurements were performed using $E_i = 35$ meV neutrons with Fermi chopper frequency at 180 Hz, which gave an energy resolution of ~ 2.7 meV (FWHM) at the elastic position. Again the same $x = 0.24$ Nd-LSCO single-crystal sample was loaded in a pumped ^{4}He magnet cryostat with a base temperature of 2 K, maximum magnetic field 8 T. The $HK0$ plane of reciprocal space of the sample was coincident with the horizontal plane. The single-crystal sample was rotated through $100°$ about its vertical axis in increments of $1°$ during the course of any one measurement, which typically required 12 h of counting time.

III. PARALLEL SPIN STRIPE ORDER PARAMETER IN ZERO FIELD IN $La_{1.6-x}Nd_{0.4}Sr_{0.24}CuO_4$

We carried out new elastic neutron scattering measurements on the same single crystal of Nd-LSCO with $x = 0.24$, as was previously studied [32]. The new measurements were performed with a higher-temperature point density and improved counting statistics, roughly four times greater than previously published data [48]. The result is the order parameter for parallel spin stripe order in Nd-LSCO, $x = 0.24$, shown in Fig. 2(b). For comparison the corresponding order parameter for $x = 0.19$ near optimal hole doping in Nd-LSCO is shown in Fig. 2(a) [32]. Both data sets are plotted on log-log scales.

As reported earlier, the order parameter at $x = 0.19$ shows an onset of nonzero intensity at 2D $T_N = 35 \pm 2$ K [32]. The relatively large separation between 2D T_N and superconducting $T_C = 13.5 \pm 1$ K allows the clear observation of an inflection point in the temperature dependence of the order parameter at T_C. In contrast, 2D $T_N = 13 \pm 1$ K, consistent with earlier measurements [32], and superconducting $T_C = 11 \pm 1$ K [23] are almost coincident for $x = 0.24$, as can be seen in Fig. 2(b). Both order parameters show a pronounced upturn in intensity below ~ 5 K, associated with the participation in ordered Nd^{3+} magnetism in the parallel spin stripe structure.

IV. MAGNETIC FIELD DEPENDENCE OF PARALLEL SPIN STRIPE ORDER IN $La_{1.6-x}Nd_{0.4}Sr_{0.24}CuO_4$ FOR $H \parallel c$

Elastic scattering order-parameter measurements on our Nd-LSCO single crystal were repeated under the application of a magnetic field $\parallel c$, for fields up to 8 T, and compared with those in zero field. A subset of these measurements, at the incommensurate parallel spin stripe wave vector (0.5, 0.64, 0) with $H \parallel c = 8$ T and as a function of temperature, are
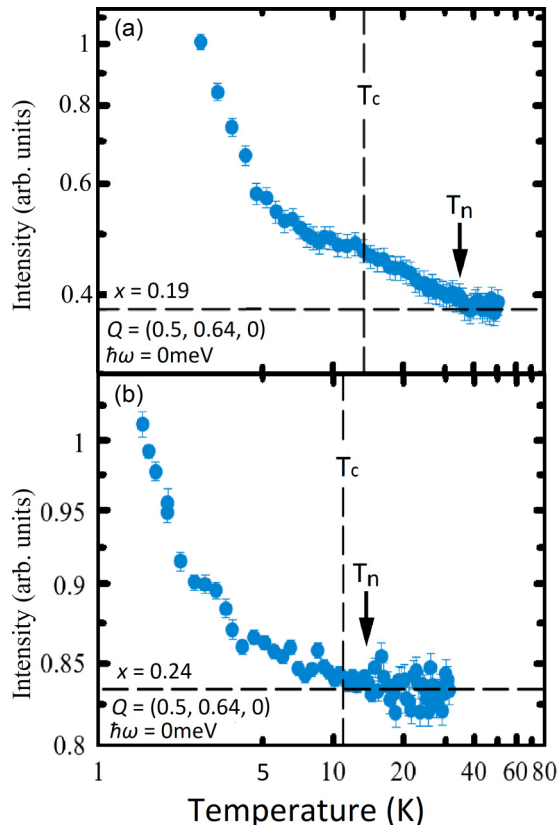
FIG. 2. The zero magnetic field order parameters taken from TAS instrument at HFIR as a function of temperature for optimal doping, $x = 0.19$, and near the pseudogap QCP, $x = 0.24$. (a) Shows elastic scattering neutron data for Nd-LSCO with $x = 0.19$ [32], while (b) shows the same data for $x = 0.24$. Fiducials are shown for both superconducting T_C and 2D T_N for each single crystal. Note that both the intensity (y) scale and the temperature (x) scales are logarithmic.
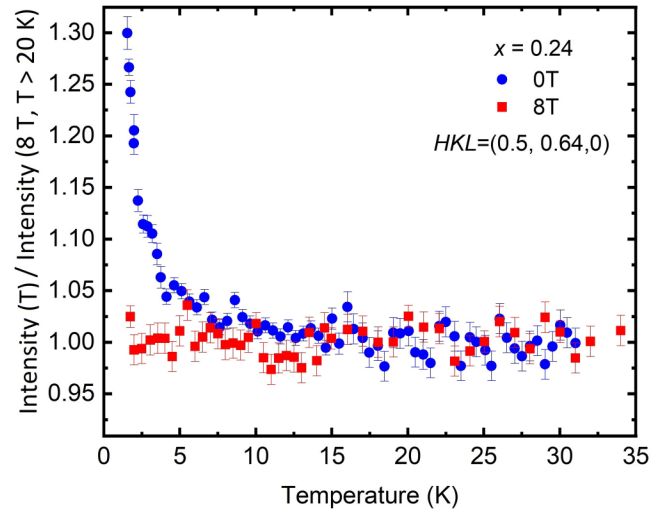

FIG. 3. The elastic neutron scattering order parameter as measured in Nd-LSCO with $x=0.24$ is shown in both $H = 0$ T (blue points) and $H \parallel c = 8$ T (red points). The order parameter is measured with neutron intensity normalized to the monitor counts which is approximately 10 min counting time. The intensity is proportional to the square of the ordered magnetic moment. The intensity and temperature scales are linear, and the intensity has been normalized to 1 at high temperatures for both 0- and 8-T data. The error bars were determined from appropriate counting statistics.

shown in Fig. 3. Here they are compared to the corresponding $H = 0$ measurements, also shown in Fig. 2(b), but now on linear scales. One can see that no temperature dependence is observed in the $H \parallel c = 8$ T data set, indicating that the elastic parallel spin stripe scattering is eliminated at 8 T. For the raw data which are only normalized to monitor counts, see Sec. II in the Supplemental Material [49].

Figure 4 shows similar elastic scattering at the incommensurate parallel spin stripe wave vector (0.5, 0.65, 0), but as a function of $H \parallel c$ at $T = 1.5$ K for the $x = 0.24$ sample. Measurements were performed both increasing and decreasing the magnetic field, and a clear hysteresis is observed for 0.2 T $\leqslant H \leqslant 0.7$ T. We take this as evidence for a first-order transition with field, which occurs at approximately the same field required to destroy parallel spin stripe order in Nd-LSCO $x = 0.15$ [46]. As can be seen from Fig. 4, the suppression of static parallel spin stripe order in $x = 0.24$ is complete by $\sim H \parallel c = 2.5$ T.

Complementary time-of-flight neutron scattering measurements were also carried out on the same single crystal of Nd-LSCO with $x = 0.24$ using the HYSPEC instrument at the Spallation Neutron Source. Figure 5(a) shows an elastic scattering map in the ($H, K, -3 \leqslant L \leqslant 3$) plane of reciprocal

space. This shows the difference between a data set at $T = 2$ K and $H \parallel c = 7$ T and a data set at $T = 2$ K and $H = 0$ T. Clear negative elastic net intensity can be observed around the $(\frac{1}{2}, \frac{1}{2}, -3 \leqslant L \leqslant 3)$ and $(\frac{3}{2}, \frac{3}{2}, -3 \leqslant L \leqslant 3)$ positions. As the time-of-flight measurements also inform on the energy dependence of the scattering, we can plot a related difference
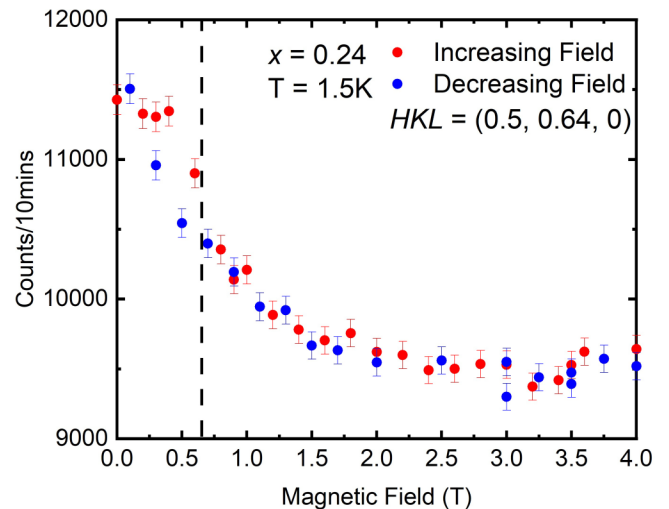

FIG. 4. The elastic neutron scattering parallel spin stripe order parameter as a function of $H \parallel c$ is shown at $T = 1.5$ K. The red points show data taken while increasing H, while the blue points show data taken on decreasing H. Note that hysteresis is present just below $H = 0.7$ T, which is marked as a vertical dashed line. This indicates a first-order-like metamagnetic transition just below $H = 0.7$ T.
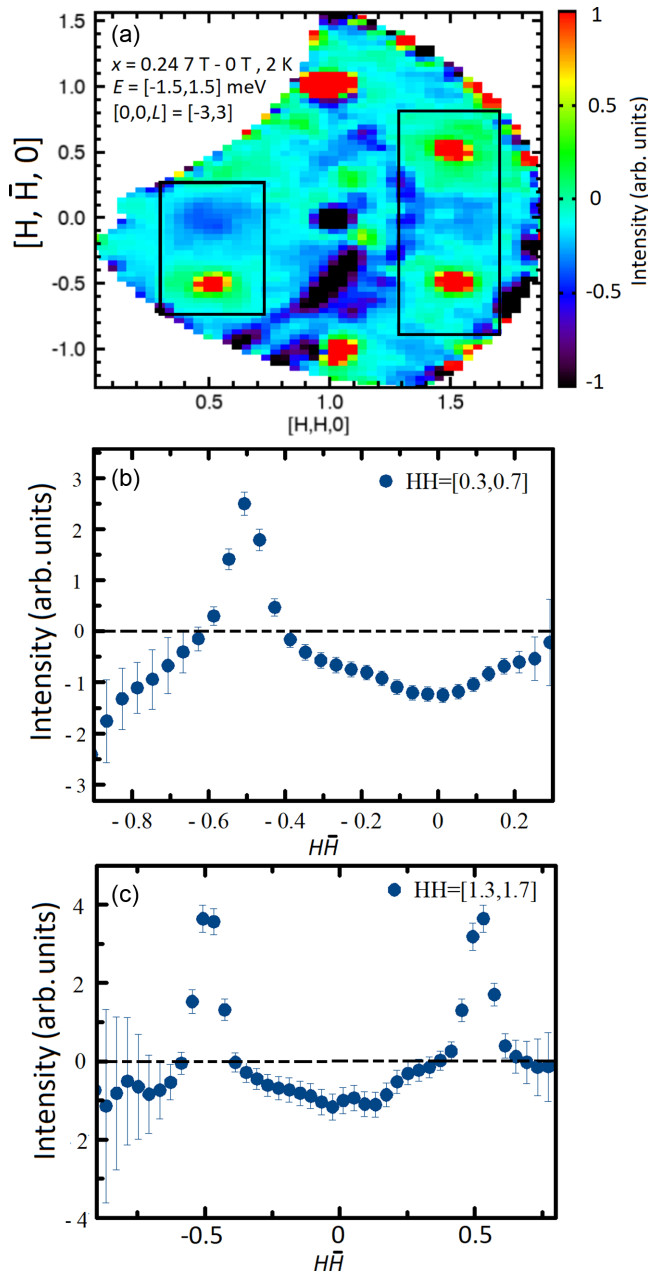
FIG. 5. (a) Shows a magnetic-field difference data set $H \parallel c = 7$ –0 T for elastic scattering (-1.5 meV $\leqslant \hbar\omega \leqslant 1.5$ meV) from time-of-flight neutron scattering in the $[H, -H, -3 \leqslant L \leqslant 3]$ scattering plane. A semicircular region with high background from Al-powder rings due to sample addenda, which do not subtract out cleanly from each other, is present in the middle of the plot. (b) Shows a vertical cut through the rectangle on the left of (a), showing a peak at the $(1,0, -3 \leqslant L \leqslant 3)$, and a valley at $(\frac{1}{2}, \frac{1}{2}, -3 \leqslant L \leqslant 3)$. (c) Shows a vertical cut through the rectangle on the right of (a), showing peaks at the $(1,2, -3 \leqslant L \leqslant 3)$ and $(2, 1, -3 \leqslant L \leqslant 3)$, with a valley at $(\frac{3}{2}, \frac{3}{2}, -3 \leqslant L \leqslant 3)$. These peaks and valleys are consistent with a magnetic-field-induced transfer of diffracted intensity from incommensurate parallel spin stripe ordering wave vectors, to commensurate wave vectors, indicating a polarization of the static spins participating in the parallel spin stripe structure on application of $H \parallel c$.

plot using these data. For the original data used to produce the difference in Figs. 5(b) and 5(c) (see Sec. I in the Supplemen-
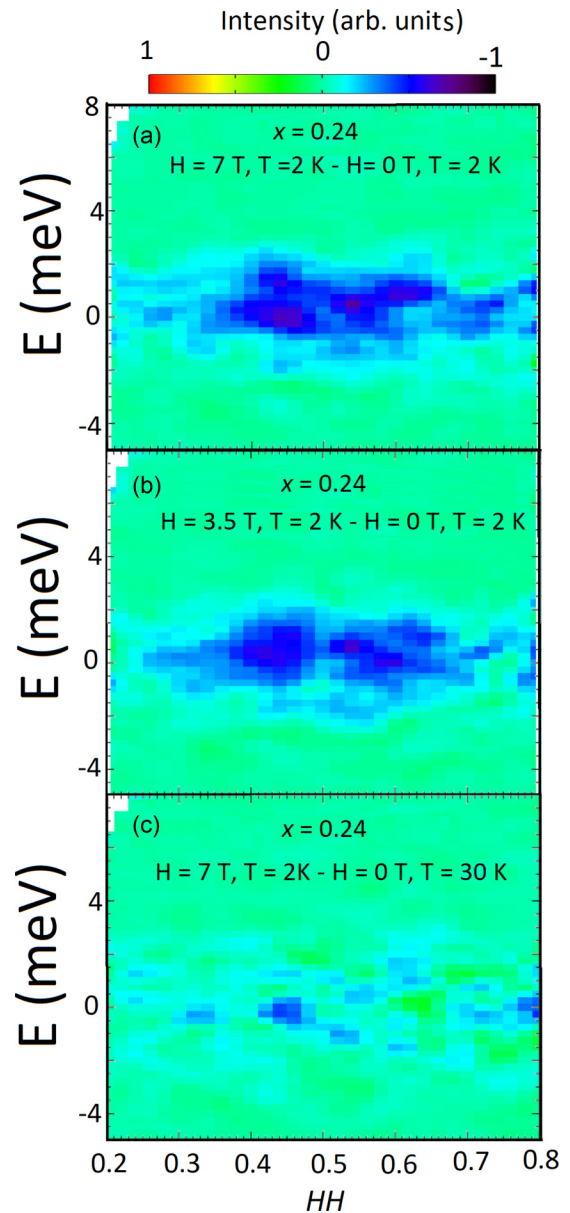

FIG. 6. (a)–(c) Show different magnetic field difference data sets for Nd-LSCO with $x = 0.24$, plotted in the energy-HH reciprocal space plane. These difference plots, made up from time-of-flight data sets, have been integrated in L from -3 to 3 and in $H\bar{H}$ from -0.1 to 0.1. (a) Shows $H = 7$–0 T, at $T = 2$ K, while (b) shows 3.5– 0 T, at $T = 2$ K. The net negative intensity around $HH = 0.4$ and 0.6 in (a) and (b) shows the suppression of the quasi-Bragg peaks due to parallel spin stripe order in an applied magnetic field $H \parallel c = 7$ and 3.5 T, respectively. (c) Shows the difference between data sets at $H = 7$ T at $T = 2$ K and $H = 0$ T at $T = 30$ K $> 2D$ T_N. Collectively, these data sets confirm that the suppression of the incommensurate parallel spin stripe quasi-Bragg peaks is complete at $H \parallel c > 2.5$ T, as also concluded from our TAS data shown in Fig. 4.

tal Material [49]). Figure 6(a) shows an $H//c = 7$ T data set with an $H = 0$ T data set subtracted from it, both at $T = 2$ K. This difference data set is now integrated in $-3 \leqslant L \leqslant 3$ and $-0.1 \leqslant H\bar{H} \leqslant 0.1$, and it is plotted as a function of energy vs the HH direction in reciprocal space in Fig. 6(a). Figure 6(b)

shows the same integrations, but the difference data are the subtraction of an $H = 0$ T data set from an $H \parallel c = 3.5$ T data set, both at $T = 2$ K. Figure 6(c) shows the subtraction of an $H = 0$ T data set for $T = 30$ K > 2D T_N from an $H \parallel c = 7$ T data set at $T = 2$ K.

Together, the HYSPEC data sets shown in Figs. 5 and 6 demonstrate that the destruction of the incommensurate elastic scattering from the parallel spin stripes is complete by $H \parallel c = 3.5$ T, consistent with the TAS data which showed complete suppression by $\sim$2.5 T. The effect of the magnetic field $\parallel c$ at $H = 7$ T is as effective as raising the temperature to $>2\times$ 2D T_N, as Fig. 6(c) demonstrates.

However, the elastic scattering survey of the $x = 0.24$ single crystal in its $(H, K, -3 \leqslant L \leqslant 3)$ plane shows more than the destruction of the static incommensurate parallel spin stripe scattering for $H \parallel c$ beyond $\sim$2.5 T. The reciprocal space map in Fig. 5(a) and cuts along $(HH0)$ in Figs. 5(b) and 5(c) show a concomitant buildup of scattering around commensurate wave vectors, such as $(0, 1, -3 \leqslant L \leqslant 3)$, $(1, 1, -3 \leqslant L \leqslant 3)$, and $(1, 2, -3 \leqslant L \leqslant 3)$. This is interpreted as the static moment participating in the parallel spin stripe structure not being destroyed, but rather being polarized by the magnetic field.

V. MEASUREMENT OF THE SPIN GAP IN La$_{1.6-x}$Nd$_{0.4}$Sr$_{0.24}$CuO$_4$ AND ITS CORRELATION WITH T_C COMPARED TO OTHER CUPRATE SUPERCONDUCTORS

Inelastic neutron scattering measurements on Nd-LSCO with $x = 0.24$ were also carried out using TAS, at the incommensurate parallel spin stripe ordering wave vector (0.5, 0.64, 0) for energies less than 11 meV. These measurements were carried out at base temperature $T = 1.5$ K in both $H = 0$ and 8 T $\parallel c$. Approximating the $H = 8$ T state as the normal state, we then expect the difference between the inelastic scattering measured in 8 and 0 T to identify the spin gap, as spin fluctuations less than a characteristic spin-gap energy are expected to be suppressed in the superconducting states, compared to the normal state.

These inelastic scattering data, in the 2 meV $\leqslant \hbar\omega \leqslant$ 8 meV regime, at $H = 0$ and 8 T, both at $T = 1.5$ K, are shown in Fig. 7(a). As can be seen, the inelastic scattering is systematically higher in the $H = 8$ T data set below 3 ± 0.5 meV, and this is identified as the measured spin gap Δ_{spin} for Nd-LSCO $x = 0.24$.

A similar protocol has been followed to identify Δ_{spin} in other cuprate superconductors. However, as these other cuprates have superconducting T_C's larger, and often much larger, than those of the Nd-LSCO family, the corresponding critical magnetic fields are also larger. Therefore, the normal-state spin fluctuation spectrum is measured for $T > T_C$, and the corresponding $\chi''(\mathbf{Q}, \hbar\omega) = S(\mathbf{Q}, \hbar\omega) \times [1 - \exp(\frac{-\hbar\omega}{kT})]$ is compared with the $\chi''(\mathbf{Q}, \hbar\omega)$ at low temperatures, well below T_C, in order to identify Δ_{spin}. Recent work by Li *et al.* [50] nicely illustrates this protocol for the $x = 0.17$ and 0.21 members of the LSCO family. This same work also compiles results for Δ_{spin} and T_C across five families of cuprate superconductors, with T_C's ranging from 25 to 95 K.

We can follow this same temperature protocol to estimate Δ_{spin} for Nd-LSCO $x = 0.19$, as data for $\chi''(\mathbf{Q}, \hbar\omega)$ at $T =$
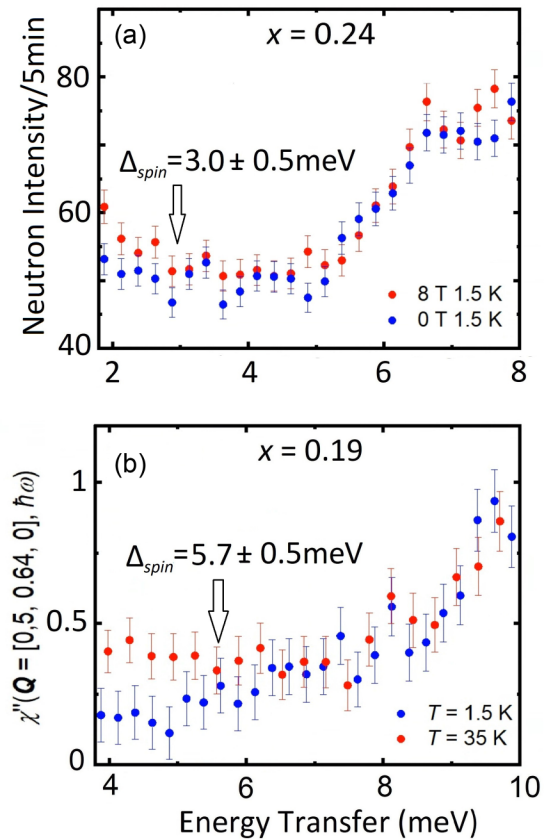

FIG. 7. (a) Inelastic neutron scattering from Nd-LSCO with $x = 0.24$ for both $H \parallel c = 8$ T and $T = 1.5$ K and $H = 0$ and $T = 1.5$ K. These TAS data are a constant $\mathbf{Q}$ scan at the (0.5, 0.64, 0) parallel spin stripe ordering wave vector. The spin gap $\Delta_{\text{spin}} = 3 \pm 0.5$ meV is identified as the energy at which inelastic scattering in the (near) normal state ($H \parallel c = 8$ T) no longer exceeds that in the superconducting state ($H = 0$). (b) $\chi''(\mathbf{Q}, \hbar\omega)$ extracted from inelastic neutron scattering, as reported in [32], is shown in zero magnetic both above, $T = 35$ K, and below, $T = 1.5$ K, superconducting T_C. $\Delta_{\text{spin}} = 6 \pm 0.5$ meV is identified as the energy at which inelastic scattering in the normal state ($T = 35$ K) no longer exceeds that in the superconducting state ($T = 1.5$ K). The universal upturn around 6 meV can be understood as the onset of the crystal electric field (CEF) scattering associated with transitions from the Nd^{3+} ground-state doublet and the first-excited-state doublet [39]. The error bar is estimated by taking a step in both directions from the point at which the high-field inelastic scattering is systematically higher by a standard error from the corresponding zero-field data in the superconducting state.

1.5 and 35 K have previously been published [32]. We plot this $\chi''(\mathbf{Q}, \hbar\omega)$ data for Nd-LSCO $x = 0.19$ in Fig. 7(b) in the 4 meV $\leqslant \hbar\omega \leqslant$ 10 meV regime. As in Fig. 7(a) for $x = 0.24$, this is a 6-meV energy range for which the low-energy spectral weight is approximately energy independent, making it relatively easy to identify a low-energy suppression of the magnetic spectral weight in the superconducting state. We identify the dip in $\chi''(\mathbf{Q}, \hbar\omega, T = 1.5$ K) below $\chi''(\mathbf{Q}, \hbar\omega, T = 35$ K) at 5.7 ± 0.5 meV as Δ_{spin}. With estimates for Δ_{spin} in hand for Nd-LSCO for $x = 0.24$ and 0.19, we can extend the Li *et al.* [50] compilation of Δ_{spin} vs T_C
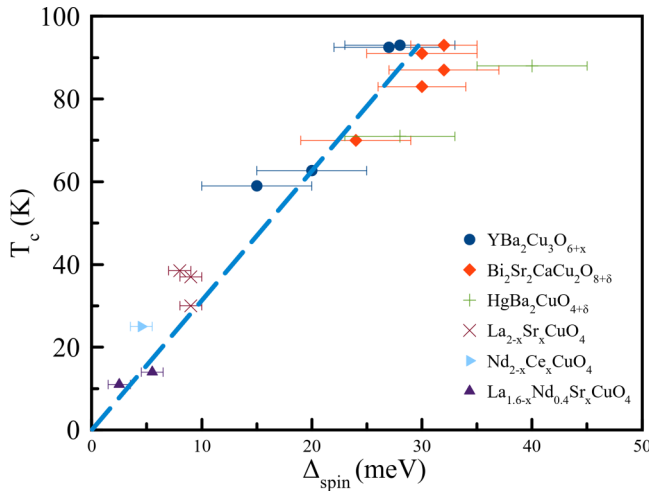
FIG. 8. A compilation of spin gap Δ_{spin} vs superconducting T_C is shown for five different families of cuprate superconductors. The data points for Nd-LSCO are for the Δ_{spin} results for $x = 0.24$ and 0.19 reported in this paper. The other data points were compiled in Li *et al.* [50]. The overall data set is well described by a linear relationship between the two, $\Delta_{\text{spin}} = 3.5 \, k_B T_C$, similar to that describing the energy gap vs T_C relation in BCS superconductors.

data for cuprate families down towards $T_C = 0$. These data are plotted in Fig. 8, along with a straight line guide to the eye, which passes through $\Delta_{\text{spin}} = 0$ $T_C = 0$. One can see that a good linear relation between Δ_{spin} and T_C, $\Delta_{\text{spin}} = 3.5 \, k_B \, T_C$, is obeyed across almost an order of magnitude in T_C.

There have been some concerns on whether the enhanced signal in Fig. 7 is due to an inelastic contribution of the spin-polarized state instead of the result of spin gap. While we can not rule out the possibility of this scenario, we make two observations that would seem to make such scenario unlikely. The transfer of elastic intensity from the incommensurate spin stripe ordering wave vectors to commensurate, ferromagnetic wave vectors (as we observed) is expected, if the effect of the magnetic field is to polarize (i.e., align) the local moments taking part in the static spin stripe order in zero field. There is no corresponding local moment argument by which low-energy, inelastic spectral weight is expected to be enhanced at the same incommensurate spin stripe wave vectors by application of a uniform field, such that the low-energy incommensurate spectral weight in the high-field state exceeds that in the zero-field, superconducting state. Second, the spin gap so identified by this protocol fits well with the trend of spin gap vs superconducting T_C, as shown in Fig. 8, for five families of cuprate-based high-temperature superconductors. Most of these (all except the 214 families) do not display elastic incommensurate spin stripe scattering. Hence, a consistent explanation is that the gap arises due to the destruction of the superconductivity, rather than the polarization of the elastic spin stripe scattering.

VI. DISCUSSION

The main result of this paper is that the static parallel spin stripe structure observed in Nd-LSCO with $x = 0.24$ below 2D $T_N = 13 \pm 1$ K in $H = 0$ T is eliminated in $H \parallel c \geqslant 2.5$ T.

On the one hand, this is a surprising result, as previous in-field diffraction studies of parallel spin stripe order have shown little or no field dependence for accessible magnetic field strengths ($\leqslant 10$ T). The previous study most similar to that reported here is the study on Nd-LSCO with $x = 0.15$ [46], underdoped but approaching optimal doping. This $x = 0.15$ study showed the elimination of the strong upturn of the parallel spin stripe order parameter below ~ 5 K by application of a magnetic field $\parallel c$. This is interpreted as the polarization of the Nd^{3+} magnetism and the removal of its influence on the low-temperature spin stripe structure. At higher temperatures in $H \parallel c = 7$ T, the $x = 0.15$ order parameter is about 20% lower than that in $H = 0$, but its 2D T_N remains ~ 40 K. Thus, the higher-temperature component of the order parameter, presumably due to Cu^{2+} magnetism alone, is only modestly diminished in a $H \parallel c = 7$ T field.

Our current results on $x = 0.24$ extend this trend significantly. Now the low-temperature upturn in the parallel spin stripe order parameter is suppressed in a first-order fashion as a function of field, with hysteresis, as Fig. 4 shows, and this initial suppression is complete by $H \parallel c \sim 0.7$ T. However, the complete elimination of the incommensurate parallel spin stripe quasi-Bragg peaks requires $H_C \parallel c \sim 2.5$ T. Thus, the static parallel spin stripe order in Nd-LSCO with $x = 0.24$ is similar to that observed in $x = 0.15$ and 0.125, in that it is characterized by almost the same incommensurate parallel spin stripe wave vector, but it is much more fragile, with 2D T_N a factor of 3 to 4 lower, and an $H_C \parallel c$ sufficiently reduced from $x = 0.15$ and 0.125, such that this effect is now observable with modest magnetic field capabilities.

It is interesting to note that while our elastic neutron scattering measurements of parallel spin stripes in zero magnetic field do not obviously reflect a pseudogap QCP, elastic neutron scattering in low but finite magnetic field may show exactly that: The disappearance of magnetic-field-robust parallel spin stripe order near $x^* = 0.23$.

An important corollary to the observed field dependence of the static parallel spin stripe order in Nd-LSCO $x = 0.24$ is that in-field transport and thermodynamic measurements for samples beyond optimal doping, such as those reported in [22] and [51], are not expected to see spin stripe order as the same magnetic fields required to overcome superconductivity and establish the normal state will destroy the parallel spin stripe order. As shown in Fig. 5, the static moments participating in the spin stripes structure are not destroyed, but rather appear to be polarized in modest $H \parallel c$.

Finally, we took advantage of relatively low critical field $\parallel c$ for superconductivity in order to examine the low-energy spin fluctuations at the parallel spin stripe ordering wave vector in both a superconducting ground state ($H = 0$) and in a state with most of its volume corresponding to the normal state ($H = 8$ T). This is a different protocol for identifying the spin gap Δ_{spin}, compared with the more typical protocol of looking at the spin fluctuations above and below T_C in zero field. However, the use of the field-induced normal state has the advantage that it allows all the spin fluctuation measurements to be performed at base temperature, and hence no correction for the Bose factor, which relates $S(\mathbf{Q}, \hbar\omega)$ to $\chi''(\mathbf{Q}, \hbar\omega)$, is required. The Bose factor correction is not difficult to apply, but it must be applied to $S(\mathbf{Q}, \hbar\omega)$ alone, and

thus $S(\mathbf{Q}, \hbar\omega)$ must be clearly differentiated from background scattering in order to use the temperature-difference protocol.

We have used the field protocol to estimate Δ_{spin} in the $x = 0.24$ sample, and the temperature-difference protocol to do the same for $x = 0.19$, using previously published data [32]. This allows us to add two data points at the low-field extreme of the Δ_{spin} vs T_C compilation initiated by Li *et al.* [50]. We find that these estimates fit with the linear trend between these two observables in five different families of cuprate superconductors, covering almost a decade in T_C. Remarkably, this linear relation is given by $\Delta_{\text{spin}} = 3.5 k_B T_C$, implying a role for Δ_{spin} akin to $2 \times \Delta$ as measured in tunneling experiments on BCS superconductors.

VII. CONCLUSIONS

Elastic neutron scattering measurements on single-crystal Nd-LSCO with $x = 0.24$ in the presence of a magnetic field, $H \parallel c$, show that the previously observed parallel spin stripe incommensurate quasi-Bragg peaks are reduced to zero intensity for $H \geqslant 2.5$ T. Their low-temperature enhancement below $T \sim 5$ K in $H = 0$ is eliminated in a first-order fashion with H for $H \parallel c \leqslant 0.7$ T. While the effect of the field on the low-temperature enhancement of the parallel spin stripe order parameter is consistent with earlier work at $x = 0.15$ [46], the complete elimination of the order parameter for fields above ~ 2.5 T is surprising given the lack of field dependence previously observed near $x = 0.125$ [44], and the enhancements of

the order parameter in field observed in underdoped LSCO [52]. We conclude that while the incommensurate parallel spin stripe structure in Nd-LSCO with $x = 0.24$ is similar to that exhibited in $x = 0.125$ and 0.15, it is much more easily perturbed by either temperature or magnetic field. This work has implications for transport and thermodynamic measurements made in the presence of large magnetic fields, so as to establish normal-state properties at low temperatures in Nd-LSCO at relatively high hole doping.

Low-energy inelastic neutron scattering measurements at the parallel spin stripe ordering wave vector in Nd-LSCO $x = 0.24$ in $H = 8$ T allow us to estimate a spin gap $\Delta_{\text{spin}} = 3.0 \pm 0.5$ meV. We combine this result, with an analysis on preexisting Nd-LSCO $x = 0.19$ data, to fill out the low-T_C region of a Δ_{spin} vs T_C compilation across five families of cuprate superconductors, and observe a linear relationship between them. Intriguingly, this relationship is roughly given by $\Delta_{\text{spin}} = 3.5 k_B T_C$.

[1] J. G. Bednorz and K. A. Müller, Possible high T_c superconductivity in the Ba-La-Cu-O system, Z. Phys. B **64**, 189 (1986).

[2] M. K. Wu, J. R. Ashburn, C. J. Torng, P. H. Hor, R. L. Meng, L. Gao, Z. J. Huang, Y. Q. Wang, and C. W. Chu, Superconductivity at 93 K in a New Mixed-Phase Y-Ba-Cu-O Compound System at Ambient Pressure, Phys. Rev. Lett. **58**, 908 (1987).

[3] P. W. Anderson, The resonating valence bond state in La$_2$CuO$_4$ and superconductivity, Science **235**, 1196 (1987).

[4] V. J. Emery, Theory of High-T_c Superconductivity in Oxides, Phys. Rev. Lett. **58**, 2794 (1987).

[5] L. C. Bourne, A. Zettl, T. W. Barbee, III, and M. L. Cohen, Complete absence of isotope effect in YBa$_2$Cu$_3$O$_7$: Consequences for phonon-mediated superconductivity, Phys. Rev. B **36**, 3990 (1987).

[6] G. Kotliar and J. Liu, Superexchange mechanism and d-wave superconductivity, Phys. Rev. B **38**, 5142 (1988).

[7] J. R. Schrieffer, X.-G. Wen, and S.-C. Zhang, Spin-Bag Mechanism of High-Temperature Superconductivity, Phys. Rev. Lett. **60**, 944 (1988).

[8] F. C. Zhang and T. M. Rice, Effective hamilton for the superconducting Cu oxides, Phys. Rev. B **37**, 3759 (1988).

[9] J. P. Franck, Experimental Studies of the Isotope Effect in High Temperature Superconductors, *in Physical Properties of High Temperature Superconductors IV* (World Scientific, Singapore, 1994), Chap. 4, p. 189.

[10] V. J. Emery, S. A. Kivelson, and O. Zachar, Spin-gap proximity effect mechanism of high-temperature superconductivity, Phys. Rev. B **56**, 6120 (1997).

[11] M. L. Kulić, Interplay of electron–phonon interaction and strong correlations: The possible way to high-

temperature superconductivity, Phys. Rep. **338**, 1 (2000).

[12] P. A. Lee, N. Nagaosa, and X.-G. Wen, Doping a mott insulator: Physics of high-temperature superconductivity, Rev. Mod. Phys. **78**, 17 (2006).

[13] H. Mukuda, S. Shimizu, A. Iyo, and Y. Kitaoka, High-T_c superconductivity and antiferromagnetism in multilayered copper oxides: New paradigm of superconducting mechanism, J. Phys. Soc. Jpn. **81**, 011008 (2012).

[14] D. J. Scalapino, A common thread: The pairing interaction for unconventional superconductors, Rev. Mod. Phys. **84**, 1383 (2012).

[15] L. Taillefer, Scattering and pairing in cuprate superconductors, Annu. Rev. Condens. Matter Phys. **1**, 51 (2010).

[16] C. Proust and L. Taillefer, The remarkable underlying ground states of cuprate superconductors, Annu. Rev. Condens. Matter Phys. **10**, 409 (2019).

[17] J. M. Tranquada, Spins, stripes, and superconductivity in hole-doped cuprates, in *Lectures on the Physics of Strongly Correlated systems XVII: Seventeenth Training Course in the Physics of Strongly Correlated Systems*, edited by A. Avella and F. Mancin, AIP Conf. Proc. 1550 (AIP, Melville, NY, 2013), pp. 114–187.

[18] J. M. Tranquada, Cuprate superconductors as viewed through a striped lens, Adv. Phys. **69**, 437 (2020).

[19] M. A. Kastner, R. J. Birgeneau, G. Shirane, and Y. Endoh, Magnetic, transport, and optical properties of monolayer copper oxides, Rev. Mod. Phys. **70**, 897 (1998).

[20] B. Keimer, N. Belk, R. J. Birgeneau, A. Cassanho, C. Y. Chen, M. Greven, M. A. Kastner, A. Aharony, Y. Endoh, R. W.

Erwin, and G. Shirane, Magnetic excitations in pure, lightly doped, and weakly metallic La$_2$CuO$_4$, Phys. Rev. B **46**, 14034 (1992).

[21] J. M. Tranquada, B. J. Sternlieb, J. D. Axe, Y. Nakamura, and S. Uchida, Evidence for stripe correlations of spins and holes in copper oxide superconductors, Nature (London) **375**, 561 (1995).

[22] B. Michon, C. Girod, S. Badoux, J. Kačmarčík, Q. Ma, M. Dragomir, H. A. Dabkowska, B. D. Gaulin, J.-S. Zhou, S. Pyon, T. Takayama, H. Takagi, S. Verret, N. Doiron-Leyraud, C. Marcenat, L. Taillefer, and T. Klein, Thermodynamic signatures of quantum criticality in cuprate superconductors, Nature (London) **567**, 218 (2019).

[23] M. Dragomir, Q. Ma, J. P. Clancy, A. Ataei, P. A. Dube, S. Sharma, A. Huq, H. A. Dabkowska, L. Taillefer, and B. D. Gaulin, Materials preparation, single-crystal growth, and the phase diagram of the cuprate high-temperature superconductor La$_{1.6-x}$Nd$_{0.4}$Sr$_x$CuO$_4$, Phys. Rev. Mater. **4**, 114801 (2020).

[24] J. Zaanen and O. Gunnarsson, Charged magnetic domain lines and the magnetism of high-T_c oxides, Phys. Rev. B **40**, 7391 (1989).

[25] S.-W. Cheong, G. Aeppli, T. E. Mason, H. Mook, S. M. Hayden, P. C. Canfield, Z. Fisk, K. N. Clausen, and J. L. Martinez, Incommensurate Magnetic Fluctuations in La$_{2-x}$Sr$_x$CuO$_4$, Phys. Rev. Lett. **67**, 1791 (1991).

[26] O. Zachar, S. A. Kivelson, and V. J. Emery, Landau theory of stripe phases in cuprates and nickelates, Phys. Rev. B **57**, 1422 (1998).

[27] L. Nie, A. V. Maharaj, E. Fradkin, and S. A. Kivelson, Vestigial nematicity from spin and/or charge order in the cuprates, Phys. Rev. B **96**, 085142 (2017).

[28] S. Lee, E. W. Huang, T. A. Johnson, X. Guo, A. A. Husain, M. Mitrano, K. Lu, A. V. Zakrzewski, G. A. de la Peña, Y. Peng *et al.*, Generic character of charge and spin density waves in superconducting cuprates, PNAS **119**, e2119429119 (2022).

[29] S. Wakimoto, G. Shirane, Y. Endoh, K. Hirota, S. Ueki, K. Yamada, R. J. Birgeneau, M. A. Kastner, Y. S. Lee, P. M. Gehring, and S. H. Lee, Observation of incommensurate magnetic correlations at the lower critical concentration for superconductivity in La$_{2-x}$Sr$_x$CuO$_4$ (x = 0.05), Phys. Rev. B **60**, R769 (1999).

[30] S. R. Dunsiger, Y. Zhao, B. D. Gaulin, Y. Qiu, P. Bourges, Y. Sidis, J. R. D. Copley, A. Kallin, E. M. Mazurek, and H. A. Dabkowska, Diagonal and collinear incommensurate spin structures in underdoped La$_{2-x}$Ba$_x$CuO$_4$, Phys. Rev. B **78**, 092507 (2008).

[31] S. R. Dunsiger, Y. Zhao, Z. Yamani, W. J. L. Buyers, H. A. Dabkowska, and B. D. Gaulin, Incommensurate spin ordering and fluctuations in underdoped La$_{2-x}$Ba$_x$CuO$_4$, Phys. Rev. B **77**, 224410 (2008).

[32] Q. Ma, K. C. Rule, Z. W. Cronkwright, M. Dragomir, G. Mitchell, E. M. Smith, S. Chi, A. I. Kolesnikov, M. B. Stone, and B. D. Gaulin, Parallel spin stripes and their coexistence with superconducting ground states at optimal and high doping in La$_{1.6-x}$Nd$_{0.4}$Sr$_x$CuO$_4$, Phys. Rev. Res. **3**, 023151 (2021).

[33] K. Yamada, C. H. Lee, K. Kurahashi, J. Wada, S. Wakimoto, S. Ueki, H. Kimura, Y. Endoh, S. Hosoya, G. Shirane, R. J. Birgeneau, M. Greven, M. A. Kastner, and Y. J. Kim, Doping dependence of the spatially modulated dynamical spin correla-

tions and the superconducting-transition temperature in La$_{2-x}$Sr$_x$CuO$_4$, Phys. Rev. B **57**, 6165 (1998).

[34] O. Cyr-Choinière, R. Daou, J. Chang, F. Laliberté, N. Doiron-Leyraud, D. LeBoeuf, Y. J. Jo, L. Balicas, J.-Q. Yan, J.-G. Cheng, J.-S. Zhou, J. B. Goodenough, and L. Taillefer, Zooming on the quantum critical point in nd-lsco, Phys. C (Amsterdam) **470**, S12 (2010), Proceedings of the 9th International Conference on Materials and Mechanisms of Superconductivity.

[35] R. Daou, N. Doiron-Leyraud, D. LeBoeuf, SY Li, F. Laliberté, O. Cyr-Choiniere, Y. J. Jo, L. Balicas, J.-Q. Yan, J.-S. Zhou *et al.*, Linear temperature dependence of resistivity and change in the fermi surface at the pseudogap critical point of a high-T$_c$ superconductor, Nat. Phys. **5**, 31 (2009).

[36] S. Badoux, W. Tabis, F. Laliberté, G. Grissonnanche, B. Vignolle, D. Vignolles, J. Béard, D. A. Bonn, W. N. Hardy, R. Liang, N. Doiron-Leyraud, L. Taillefer, and C. Proust, Change of carrier density at the pseudogap critical point of a cuprate superconductor, Nature (London) **531**, 210 (2016).

[37] C. E. Matt, C. G. Fatuzzo, Y. Sassa, M. Månsson, S. Fatale, V. Bitetta, X. Shi, S. Pailhès, M. H. Berntsen, T. Kurosawa, M. Oda, N. Momono, O. J. Lipscombe, S. M. Hayden, J.-Q. Yan, J.-S. Zhou, J. B. Goodenough, S. Pyon, T. Takayama, H. Takagi *et al.*, Electron scattering, charge order, and pseudogap physics in La$_{1.6-x}$Nd$_{0.4}$Sr$_x$CuO$_4$: An angle-resolved photoemission spectroscopy study, Phys. Rev. B **92**, 134524 (2015).

[38] A. Damascelli, Z. Hussain, and Z.-X. Shen, Angle-resolved photoemission studies of the cuprate superconductors, Rev. Mod. Phys. **75**, 473 (2003).

[39] Q. Ma, E. M. Smith, Z. W. Cronkwright, M. Dragomir, G. Mitchell, A. I. Kolesnikov, M. B. Stone, and B. D. Gaulin, Dynamic parallel spin stripes from the 1/8 anomaly to the end of superconductivity in La$_{1.6-x}$Nd$_{0.4}$Sr$_x$CuO$_4$, Phys. Rev. Res. **4**, 013175 (2022).

[40] S. Wakimoto, H. Zhang, K. Yamada, I. Swainson, H. Kim, and R. J. Birgeneau, Direct Relation Between the lOw-Energy Spin Excitations and Superconductivity of Overdoped High-T_c Superconductors, Phys. Rev. Lett. **92**, 217004 (2004).

[41] S. Wakimoto, K. Yamada, J. M. Tranquada, C. D. Frost, R. J. Birgeneau, and H. Zhang, Disappearance of Antiferromagnetic Spin Excitations in Overdoped La$_{2-x}$Sr$_x$CuO$_4$, Phys. Rev. Lett. **98**, 247003 (2007).

[42] B. Lake, H. M. Rønnow, N. B. Christensen, G. Aeppli, K. Lefmann, D. F. McMorrow, P. Vorderwisch, P. Smeibidl, N. Mangkorntong, T. Sasagawa *et al.*, Antiferromagnetic order induced by an applied magnetic field in a high-temperature superconductor, Nature (London) **415**, 299 (2002).

[43] E. Demler, W. Hanke, and S.-C. Zhang, *SO*(5) theory of antiferromagnetism and superconductivity, Rev. Mod. Phys. **76**, 909 (2004).

[44] J. Chang, Ch. Niedermayer, R. Gilardi, N. B. Christensen, H. M. Rønnow, D. F. McMorrow, M. Ay, J. Stahn, O. Sobolev, A. Hiess, S. Pailhes, C. Baines, N. Momono, M. Oda, M. Ido, and J. Mesot, Tuning competing orders in La$_{2-x}$Sr$_x$CuO$_4$ cuprate superconductors by the application of an external magnetic field, Phys. Rev. B **78**, 104525 (2008).

[45] J. Wen, Z. Xu, G. Xu, J. M. Tranquada, G. Gu, S. Chang, and H. J. Kang, Magnetic field induced enhancement of spin-order peak intensity in La$_{1.875}$Ba$_{0.125}$CuO$_4$, Phys. Rev. B **78**, 212506 (2008).

[46] S. Wakimoto, R. J. Birgeneau, Y. Fujimaki, N. Ichikawa, T. Kasuga, Y. J. Kim, K. M. Kojima, S.-H. Lee, H. Niko, J. M. Tranquada, S. Uchida, and M. v. Zimmermann, Effect of a magnetic field on the spin- and charge-density-wave order in $La_{1.45}Nd_{0.4}Sr_{0.15}CuO_4$, Phys. Rev. B **67**, 184419 (2003).

[47] I. A. Zaliznyak, A. T. Savici, V. O. Garlea, B. Winn, U. Filges, J. Schneeloch, J. M. Tranquada, G. Gu, A. Wang, and C. Petrovic, Polarized neutron scattering on HYSPEC: The HYbrid SPECtrometer at SNS, in *Journal of Physics: Conference Series* Vol. 862 (IOP Publishing, Bristol, 2017), p. 012030.

[48] J. M. Tranquada, J. D. Axe, N. Ichikawa, A. R. Moodenbaugh, Y. Nakamura, and S. Uchida, Coexistence of, and Competition Between, Superconductivity and Charge-Stripe Order in $La_{1.6−x}Nd_{0.4}Sr_xCuO_4$, Phys. Rev. Lett. **78**, 338 (1997).

[49] See Supplemental Material at http://link.aps.org/supplemental/10.1103/PhysRevB.106.214427 for (i) the original data used to produce Figs. 5(b) and 5(c). (ii) The raw data of order parameter in Fig. 3, only normalized to monitor counts which is about 10 min of counting time.

[50] Y. Li, R. Zhong, M. B. Stone, A. I. Kolesnikov, G. D. Gu, I. A. Zaliznyak, and J. M. Tranquada, Low-energy antiferromagnetic spin fluctuations limit the coherent superconducting gap in cuprates, Phys. Rev. B **98**, 224508 (2018).

[51] Y. Fang, G. Grissonnanche, A. Legros, S. Verret, F. Laliberté, C. Collignon, A. Ataei, M. Dion, J. Zhou, D. Graf *et al.*, Fermi surface transformation at the pseudogap critical point of a cuprate superconductor, Nat. Phys. **18**, 558 (2022).

[52] S. Katano, M. Sato, K. Yamada, T. Suzuki, and T. Fukase, Enhancement of static antiferromagnetic correlations by magnetic field in a superconductor $La_{2−x}Sr_xCuO_4$ with $x = 0.12$, Phys. Rev. B **62**, R14677(R) (2000).